**Atmospheric
Chemistry
and Physics
Discussions**

Impact of deep convection in the tropical tropopause layer in West Africa: in-situ observations and mesoscale modelling

F. Fierli[1], E. Orlandi[1], K. S. Law[2], C. Cagnazzo[3], F. Cairo[1], C. Schiller[4], S. Borrmann[5,6], G. Didonfrancesco[7], F. Ravegnani[1], and M. Volk[8,9]

[1]Institute for Atmospheric Sciences and Climate, ISAC-CNR, Italy
[2]LATMOS-IPSL, CNRS, Paris, France
[3]CMCC, Bologna, Italy
[4]Forschungzentrum Jülich, Jülich, Germany
[5]Max Planck Institute for Chemistry, Particle Chemistry Department, Mainz, Germany
[6]Institute for Atmospheric Physics, Johannes Gutenberg University, Mainz, Germany
[7]ENEA, ACS Dept., Rome, Italy
[8]Institute for Atmospheric and Environmental Sciences, J. W. Goethe-University, Frankfurt, Germany

Title Page

Abstract | Introduction

Conclusions | References

Tables | Figures

◄◄ | ►►

◄ | ►

Back | Close

Full Screen / Esc

Printer-friendly Version

Interactive Discussion

[9]now at: Department of Physics, University of Wuppertal, Wuppertal, Germany

Correspondence to: F. Fierli (f. fierli@isac.cnr.it)

Impact of deep convection in the TTL in West Africa

F. Fierli et al.

Title Page

Abstract | Introduction

Conclusions | References

Tables | Figures

◄ | ►

◄ | ►

Back | Close

Full Screen / Esc

Printer-friendly Version

Interactive Discussion

Abstract

We present the analysis of the impact of convection on the composition of the tropical tropopause layer region (TTL) in West-Africa during the AMMA-SCOUT campaign. Geophysica M55 aircraft observations of water vapor, ozone, aerosol and CO_2 show
perturbed values at altitudes ranging from 14 km to 17 km (above the main convective outflow) and satellite data indicates that air detrainment is likely originated from convective cloud east of the flight. Simulations of the BOLAM mesoscale model, nudged with infrared radiance temperatures, are used to estimate the convective impact in the upper troposphere and to assess the fraction of air processed by convection. The analysis shows that BOLAM correctly reproduces the location and the vertical structure of convective outflow. Model-aided analysis indicates that in the outflow of a large convective system, deep convection can largely modify chemical composition and aerosol distribution up to the tropical tropopause. Model analysis also shows that, on average, deep convection occurring in the entire Sahelian transect (up to 2000 km E of the measurement area) has a non negligible role in determining TTL composition.

1 Introduction

The role of deep convection and of large scale transport in determining the composition of the upper troposphere region is still a question of debate. The height where convection dominates is an important question to answer, since it impacts substantially the chemical composition, hence the radiative equilibrium in the tropical tropopause layer (TTL) (Fueglistaler, 2009; Corti et al., 2006). Several studies (see for instance Folkins and Martin, 2005; Fueglistaler and Fu, 2006) pointed out that TTL composition is controlled by slow upwelling driven by radiation, while convection determines the composition up to the lower boundary of the TTL (350 K in potential temperature coordinates) through fast vertical transport. The determination of the height of convective clouds and their subsequent impact on TTL composition is difficult to achieve from satellite

measurements due to the low sensitivity of observed parameters from, for example METEOSAT, at the tropical tropopause due to the limited vertical resolution of satellite-borne profilers. The information on the height where deep convection outflow occurs and modifies the water vapour and trace gas distributions can be derived from in-situ observations that offer an adequate vertical resolution. Several observational analyses based on in-situ aircraft data show that deep convection can impact up to the tropical tropopause (Dessler, 2002). Locally, convection can overshoot up to the lower stratosphere influencing directly the water budget above the tropopause as observed during the convective season in Brasil (Chaboureau et al., 2007), above the Hector convective system in Northern Australia (Corti et al., 2008), and in West Africa (Khaykin, 2009). The role of convection in West Africa is still poorly known; local convection superimposes its signature on the large scale circulation that is characterized by a easterly jet that transports air in the UT-LS from the Indian Ocean where deep convection in Indian Monsoon area occurs (Barret et al., 2008). A large field campaign in the framework of AMMA (African Monsoon Multidisciplinary; Redelsperger et al., 2006) was devoted to the study of the dynamics and chemical composition of atmosphere in West Africa and, in August 2006, a specific observational activity focused on the TTL based on the M55-Geophysica observations took place (Cairo et al., 2009). The meterological situation and phases of convective activity during 2006 wet season have been described in detail by Janicot et al. (2008). Ancellet et al. (2009) analysed the role of local convection on tropospheric aircraft observations and concluded that convective transport played a role in governing concentrations of ozone and other chemical tracers during the wet season up to 250 hPa in August 2006. Signatures of convection can be identified as deviations of tracer concentrations from mean profile due to rapid vertical transport from the planetary boundary layer; several typologies of air masses have been identified with highly variables values of CO and O_3 concentrations depending on the emissions in the region where convection occured and subsequent chemical processing in the upper troposphere. West Africa is characterized by the presence of potentially important and poorly known sources of aerosol and ozone precursors. Large latitudinal variability

Impact of deep convection in the TTL in West Africa

F. Fierli et al.

Full Screen / Esc

Printer-friendly Version

Interactive Discussion

of nitrogen oxides emission in West Africa during the wet season was observed during AMMA and is reported by Stewart et al. (2008); NO_x levels in the Sahelian area are high leading to higher ozone concentrations (Saunois et al., 2009) while ozone precursors from biomass burning in the southern hemispheric African continent can be transported by deep convection in the upper troposphere up to 10° N (Mari et al., 2008; Real et al., 2009). A companion paper (Law et al., 2010) presents the analysis of transport based on European Center for Medium Range Weather Forecast (ECMWF) data showing that large scale transport plays a pivotal role in determining the average vertical distribution in the Upper Troposphere Lower Stratosphere region (UTLS) over West Africa while local convection has a dominant impact up to the lower boundary of the TTL (on average 180 hPa); airmasses are lifted from the troposphere in the Indian Ocean and warm pool region and then advected westward by the tropical easterly jet. Schiller et al. (2009) analysed satellite observations coupled to a Lagrangian transport model showing that average values of water vapour in the UTLS appear to be controlled by large-scale transport. Nevertheless, the analysis of aircraft and balloon-borne observations indicates that local convection, i.e. convection formed in the Sahelian region extending from Sudan to West Africa between 10° N and 15° N, are likely to be superimposed on this zonal transport and directly influence the composition in the tropical upper troposphere above 200 hPa over West Africa and downwind. Law (2010) gives some indications of large scale organised uplift estimated from trajectories based on large scale analyses, that likely underestimates the effects of local convection while here, we use trajectories calculated from a mesoscale model to investigate the role of convective uplift on trace gas and aerosol concentrations over West Africa during August 2006. The analysis is restricted to flights where there was potentially a strong influence from local convection and data collected on these specific flights is used to examine whether signatures of local deep convection can be seen in the chemical data. Moreover, the mesoscale simulations are used to estimate the variability in convective outflow through the use of the in-situ observations coupled to the trajectory analysis. In order: (1) to evaluate the capability of the model to reproduce the vertical structure

of convective outflow and the presence of convectively processed layers above 355 K and, (2) to identify the extent of such layers and compare with the observed impact of convection in the upper troposphere. In this respect these approaches are complementary with Law (2010) providing the large-scale picture, and this paper examining the role of local deep convection in more detail.

2 Observations

The M55 Geophysica aircraft performed 5 local flights and 2 transfer flights in West Africa from 1 August to 16 August 2006. The objective was to characterize the TTL composition under different regimes (local convection, background, large scale westerly flow, and long-range transport of biomass burning emissions) and here we focus on obervations from flights on 7, 8 and 11 August, carried out in convective outflow.

Law (2010) reports the analysis of average profiles of aerosol and chemical tracers during the whole M55 campaign coupled to synoptic backtrajectories showing that during these days there was a presence of organized convective systems either close to the flights or upwind over eastern and central Africa with a likely impact in the observed upper tropospheric composition. In the following subsections we present the satellite observations of deep convection during the M55 flights and the observed vertical profiles of aerosol and chemical tracers for each one of the three selected flights.

2.1 Satellite observations

Cloud Top Brightness Temperature (CTBT) at 10.8 µm measured by the Meteosat Second Generation satellite (MSG) provides information about Mesoscale Convective System (MCS) lifetimes and positions. Figure 1 shows the evolution of MCSs before each M55 flight. A temperature threshold (CTBT<210 K) was applied to select deep convective clouds (Schmetz et al., 1997). CTBT evolution during 24 h before the observations

ACPD

10, 4927–4961, 2010

Impact of deep convection in the TTL in West Africa

F. Fierli et al.

Title Page

Abstract | Introduction

Conclusions | References

Tables | Figures

◄ | ►|

◄ | ►

Back | Close

Full Screen / Esc

Printer-friendly Version

Interactive Discussion

are reported with time resolution of 6 h and horizontal resolution of 4 km together with the M55 flight path.

2.1.1   7 August 2006

The top panel in Fig. 1 shows the MSG CTBT evolution from 6 August at 15:00 UTC to 7 August at the same time. Four MCSs, identified as organized convection, are visible during this period: (1) a first one propagating north of the measurement area; (2) and (3) two systems crossing and merging above south-west Chad; and a last one (4) in Sudan. Furthermore, sparse convection (5) develops at the boundary between Niger and Nigeria from 24 to 12 h before the observations. Assuming an average wind speed of 19 m/s derived from ECMWF analyses, it is possible to argue that the region where the M55 flew could have been influenced both by the simultaneous local convection (1) and by sparse convection (5) that occurred between 12 and 24 h before the flight above Niger.

2.1.2   8 August 2006

The CTBTs prior to 8 August flight are shown in middle panel of Fig. 1. Two MCSs formed between 7 August and 8 August, one dissolving between Sudan and Chad 12 h before measurements (1) and the second (2) dissolving over South Niger 10 h before the measurement. In that case, the mean zonal wind speed from ECMWF is 16 m/s, and it is possible to argue that the outflow of system (2) could have reached the M55 area at the time of the measurement. Furthermore, less organized convection forms at the same time of M55 observations on both the east and west sides of the flight path.

2.1.3   11 August 2006

The CTBTs before the 11 August flight are shown in bottom panel of Fig. 1. Two vast MCSs are observed: a westward moving one (1) crossing the measurements area 6 h before the flight, and an eastward one (2) dissolving over eastern Nigeria, 9 h before

Title Page

Abstract   Introduction

Conclusions   References

Tables   Figures

◄   ►►

◄   ►

Back   Close

Full Screen / Esc

Printer-friendly Version

Interactive Discussion

measurements. Using a mean zonal wind speed of 13 m/s, it is possible to argue that M55 likely sampled the outflow of system (1).

2.2 M55 observations

In this work observations of aerosol backscatter ratio (BSR), aerosol depolarization (D), ozone (O_3), water vapour (H_2O), carbon dioxide (CO_2) and particles fine fraction (N_{6-14}) from 7, 8 and 11 August 2006 are presented. Relative humidity with respect to ice freezing (RHI) is estimated from observed H_2O, temperature and pressure using the formula prescribed by the World Meteorological Organization and the Marti and Mauersberger (1993) formula for saturation pressure over ice. The description of the campaign and the overview of each flight is provided in Cairo et al. (2009) where a list of available observations are presented. Enhanced values of BSR indicate the presence of aerosols and values of D above 10% indicate the presence of particles in solid phase (Cairo et al., 1999). The mechanism of cirrus formation in the uppermost troposphere is still matter of debate, in particular whether ice particles formation can be directly linked to deep convective systems (see for instance Pfister et al., 2001 and Mace et al., 2006). The use of ice particles as tracer for convection may be ambiguous.

Ultrafine particles (N_{6-14}) are estimated as the difference between the concentration of particles larger than 6 nm and larger than 14 nm; enhanced values of N_{6-14} (up to 1000 cm^{-3}) indicate that formation must be recent because nucleation mode particles exist only for few hours to one day. Such values can be observed in recent outflow of deep convective clouds (Curtius, 2006). Observations of O_3, H_2O, CO_2 in air masses possibly influenced by local convection can be identified as deviations with respect to their average value assuming that air masses uplifted by convection are characterized by tracer concentrations close to those representative of the lower troposphere (Bertram et al., 2007). Alternatively, convective processing can act as an ozone source through lightning activity. As outlined in the introduction and discussed in Law (2010), O_3 in the UT can come from advection of pollutants sources so in that respect, and because of its lifetime, identification of local convection signature is not straightforward.

Impact of deep convection in the TTL in West Africa

F. Fierli et al.

Full Screen / Esc

Printer-friendly Version

Interactive Discussion

Non convective average profile, used to identify observed outliers, was calculated from data collected on the 4 and 13 August flights. These flights were large-scale north-south transects and provide information on the background conditions in the uppermost troposphere as shown by Law (2010) where background observations are compared to average convective profiles. Further analysis of CO_2 M55 observations during AMMA is provided by Homan et al. (2009).

Figure 2 shows the M55 observations on 7 August; there and in the following Figs. 3 and 4 dashed lines represent non-convective average profile; the flight was carried out between 11° N and 13° N and sampled a region east of the MCSs indicated by (1) in the upper panel of Fig. 1. Two layers of enhanced aerosol depolarization were observed at 350 and 370 K. Observations with enhanced aerosol concentrations (BSR>1.2) are labeled with open triangles. It can be seen that particles are in solid phase since D is larger than 20% when BSR is enhanced. Total water is enhanced with respect to the average profile in both aerosol layers where RHI exceeds 100%. O_3 concentrations range between 45 and 60 ppbv at 350 K (where BSR is enhanced) and increases steadily above 360 K. N_{6-14} shows enhanced values (above $100 \, cm^{-3}$) in the lower aerosol layer. In the higher layer, enhanced BSR were observed together with O_3 concentrations of 80 ppbv which is above the values measured below 360 K. CO_2 data were not available for this event.

Figure 3 shows the observations for 8 August; the M55 performed a north-south cross section between 8° N and 18° N (see Fig. 1, middle panel), and measurements are likely to have been influenced by MCS outflow 10 to 20 h prior to observation. Enhanced BSR and D were observed between 11° N and 14° N below 355 K, at 17° N at 365 K and at lower latitudes (11° N) between 370 and 375 K. In the lower layer, H_2O concentrations are much larger (15 to 200 ppmv) at 14° N with respect to 11° N. Values of RHI are above 100% inside the three aerosol layers. O_3 shows again a constant profile below 360 K with concentrations ranging between 40 and 70 ppbv in correspondance to the enhanced BSR (triangles). Higher concentrations of ozone are seen above. CO_2 concentrations are quite variable below 350 K (larger values at

11° N than at 14° N) and steadily increase above. Slightly reduced CO_2 concentrations were observed between 365 and 375 K. This could be interpreted as a signature of convective outflow that transport depleted CO_2 from below since convection uplifts air poor in CO_2 originating from the surface (Park et al., 2007). The aerosol layer at 365 K is also associated with enhanced H_2O (15 ppmv) and saturated RHI. No clear signature on CO_2, CO and O_3 is visible. The highest layer at 372 K is associated with enhanced H_2O and RHI>100% while CO_2 do not show any deviation with respect to the average profile. N_{6-14} cannot be estimated since observations have a partial coverage. However the analysis of total number of particles available above 360 K height do not show any increase in concentration due to nucleation event.

Figure 4 shows the observations for 11 August, taken between 12∘ N and 16∘ N (see Fig. 1, bottom panel). Several layers with enhanced BSR and D are observed up to 376 K. H_2O is enhanced in the 355–365 K layer at 18° N of latitude where no particles were observed while RHI were unsaturated. Increased H_2O was also observed between 365 and 380 K at 14° N of latitude at the same time as enhanced ice particles. N_{6-14} is higher (with values between 100 and 3000 cm^{-3}) up to 370 K and larger values are observed with background BSR. Moreover, large N_{6-14} is in general correlated to depleted CO_2. O_3 concentrations range between 45 and 60 ppbv below 355 K. Between 355 and 370 K O_3 is highly variable (45 to 90 ppbv) depending on the sampled latitude and increses steadily above that level. CO_2 shows constant concentrations below 355 K (377 ppbv) and reduced concentrations (374 ppbv) from 355 to 368 K.

From the data collected during these 3 flights, it is evident that convective impact is visible below 355 K with simultaneous enhancements in water vapour, BSR and aerosol fine fraction, together with reduced concentrations of CO_2 and nearly-constant O_3. Enhanced concentration of ice particles were also observed up to these altitudes indicating that in the main outflow they were formed as a result of deep convection. Above 355 K several layers of particles under saturated conditions were observed. During 7 and 8 August these layers were less ubiquitous with respect to the main outflow below 355 K and were, on average, not correlated to a clear signature on chemical

tracers. Nevertheless, small and sporadic signatures in CO_2 (and NO – not reported here) were observed above the main convective outflow level. Observations on 11 August show a different picture with ice aerosol observed throughout the vertical profile up to 375 K. In this case, convective impact reached up to 365 and 370 K based on the presence of reduced CO_2 concentrations and the presence of ultrafine particles. The identification of convective signatures in O_3 is less straightforward due to high ozone variability in West Africa troposphere. As discussed further in Law (2010) local sources of O_3 over West Africa which can be convectively uplifted are mixed with air masses advected from upwind regions and air from the lower stratosphere in the upper TTL. Observations of ice particles and outliers in chemical species (and ultrafine particles) are often uncorrelated in the layer between the average convective outflow at 355 K and the tropopause, leading to the qualitative conclusion that this region is composed of airmasses with different processing and lifetime in the TTL. To quantify the convective transport during the M55 observations we will use a mesoscale model as detailed below.

3 Mesoscale simulations

BOLAM (BOlogna Limited Area Model) is a meteorological mesoscale model based on primitive equations in the hydrostatic approximation and uses wind components u and v, potential temperature θ, specific humidity q and surface pressure p_s and includes the advection of passive tracers. Variables are defined on hybrid coordinates and they are distributed on a non-uniformly spaced Lorenz grid. The horizontal discretization uses geographical coodinates, with latitudinal rotation on an Arakawa C-grid. The model implements a Weighted Average Flux (WAF) scheme for the three dimensional advection. The lateral boundary conditions are imposed using a relaxation scheme that minimises wave energy reflection. Deep convection is parameterized using the scheme of Kain-Fritsch (Kain, 2004). The boundary layer scheme is based on the mixing length assumption and on the turbulent kinetic energy explicit prediction; the surface turbulent

fluxes are computed according to the Monin-Obukhov similarity theory. The parameterization of the effects of vegetation and soil processes is based on water and energy balance in a four layer soil model, and includes diagnostic computation of skin temperature and humidity, seasonally dependent vegetation effects, evapo-transpiration and interception of precipitation. The radiation is computed with a combined application of the scheme from Ritter and Geleyn (1992) and that from the operational ECMWF model (Morcrette et al., 1998). Further details about the model are given in Buzzi and Foschini (2000). The model is based on a 38 vertical level hybrid coordinate system, from the ground to the top of the atmosphere (0.1 hPa) with denser levels near the ground, leading to a vertical resolution of 800 m in the upper troposphere. The horizontal domain has 235×235 grid points or 24 km horizontal resolution. In this study, the simulation was started at 00:00 UTC on 4 August 2006 and run until 00:00 UTC on 14 August 2006. The model was continuously nudged with brightness temperatures at 10.8 μm from Meteosat Second Generation (MSG) satellite in order to accurately reproduce the evolution of mesoscale convective systems as already described in Orlandi et al. (2009).

3.1 Validation

The nudged BOLAM simulation was evaluated by comparing model derived CTBT and the satellite observations shown in Fig. 1. Figure 5 shows CTBT calculated with the RTTOV-8 (Saunders and Brunel, 2005) radiative transfer model using BOLAM water vapour, temperature and hydrometeors profiles. Similarly to Fig. 1, only regions with CTBT<210 K are plotted. BOLAM CTBTs for 7 August (shown in top panel of Fig. 5) correctly reproduce the observed evolution of MCSs labeled as 1 to 4 in Fig. 1, top panel, and also the sparse deep convection upwind of measurement area which developed 12 and 24 h before the flight took place. On the 8 August, BOLAM CTBTs (middle panel of Fig. 5) show the MCS (labeled as 1 in Fig. 1) dissolving over Niger, while MCS (2) is more scattered, particularly at the end of its life cycle, 15 to 9 h before the measurements. Furthermore, sparse and intense convection developing upwind

of the flight area 20 h before the flight is also captured by BOLAM. Bottom panel of Fig. 5 shows CTBT on 11 August. Both the position and life cycle of two MCSs are well reproduced by the model even if they appear more scattered. The nudging procedure improves the representation of convection compared with the simulation without nudg-
ing (not shown). In general, BOLAM generates less organized convective systems with respect to satellite observations but the position and the temporal evolution of MCSs are well reproduced. Simulations also show a coherent transport behavior in presence of MCSs generated by nudging, with increased divergence in the upper troposphere (Orlandi et al., 2009). Therefore, the transport by convective uplift and outflow can be
estimated from the BOLAM simulation with an accuracy considered adequate enough to be used in the interpretation of the M55 data.

3.2 Trajectories

In order to account for convective uplift, trajectories were calculated from BOLAM us-ing the on-line approach proposed by Gheusi and Stein (2002). The method is based
on the advection of air parcels positions treated as a passive tracer and the subse-quent off-line reconstruction of backward trajectories from position fields. In addition to the three-dimensional transport calculated using explicitly resolved winds, the posi-tion fields are also modified by the parametrized vertical diffusion and the convective transport that uses a mass-flux method to re-adjust the vertical displacements inside
convective clouds. Despite the uncertainties related to this approach, Gheusi and Stein (2002) have demonstrated that the Lagrangian evolution can be studied on a qualitative basis for relatively large trajectory clusters. In the present study, this method was used off-line with a time interval of 3 h to calculate the trajectories. Fierli et al. (2008) have previously shown that BOLAM trajectories provide a realistic description of the out-
flow originating from a vast convective region during the HIBISCUS (Impact of tropical convection on the upper troposphere and lower stratosphere at global scale) campaign over Brazil. Although the model vertical resolution is still fairly coarse, mesoscale model simulations are likely to resolve convective transport at altitudes ranging from the top

of the mean convection outflow and the tropopause. Two trajectory clusters were calculated for each flight. (1) Backtrajectories originating from model grid points within a region encompassing the flight path with pressure levels ranging from 300 to 100 hPa in order to include the whole upper troposphere. The overall number of trajectories varied from 6900 for 7 August, 12:00 UTC to 10 800 for 8 and 11 August. (2) Backtrajectories originating from the flight path calculated from each observation point every 5 min, leading to an average cluster of 1000 elements per each M55 flight. The results are used to identify which convective systems have generated the outflow observed by M55, and the extent to which convection might have influenced the region where observations were carried out. Based on this Lagrangian analysis, 2 different diagnostics were computed:

- The convective fraction, f_c, (calculated from cluster 2 in 12 θ layers) defined as the ratio between the number of parcels having been processed by convective uplift and the total number of trajectories. This is analogous to the model estimate of the probability that an air mass sampled by the aircraft was processed and uplifted by deep convection within a θ layer. In order to characterize the uplift, trajectories originating below 500 hPa, and uplifted with a vertical speed larger than 50 hPa/h and crossing irreversibly 250 hPa level, were selected.

- The convective age, t_c, is the time elapsed between convective uplift and observation. t_c is defined for each parcel of cluster (1,2) as the earliest time when air masses uplifted by deep convection (using the same criteria as f_c) irreversibly crossed the 250 hPa level.

f_c can be compared to similar diagnostics used to evaluate convective transport from other modeling studies such as Mullendore et al. (2005) and analysis in-situ observations (Bertram et al., 2007).

Since modeled and observed ice particle presence can also provide useful information, two additional diagnostics were defined to estimate model ice clouds and the extent to which such clouds might have been influenced by deep convection.

- The ice fraction, f^{ice}, is the fraction of points from cluster (2) with values of RHI>100% at the final point along the flight.

- The convective fraction of ice, f_c^{ice}, is the fraction of air masses uplifted by deep convection (calculated from cluster 2 using the same criteria as f_c) with values of RHI>100% at the final point along the flight.

4 Convective outflow from BOLAM trajectories

Figure 6 shows t_c estimated from backtrajectory cluster (1) initialized on 7 August, 12:00 UTC for two θ layers (369 K and 353 K). The geographical points where backtrajectories irreversibly cross the 250 hPa level are reported in the lower panel of Fig. 6 where t_c values are indicated by the colors. The number of trajectories uplifted by convection increases with decreasing altitude and the region sampled by the aircraft is marginally influenced by convection in the higher θ layer. The uplift occurred 48 to 50 h before the flight. Air masses from the lower troposphere crosses the 250 hPa level 20 to 50 h prior to the measurement; this is visible in Fig. 6 (lower panel), where it is shown that air masses irreversibly crossed 250 hPa near to deep convective systems above southern Niger and northern Nigeria. It is important to note that BOLAM does not show air masses with low t_c uplifted in the western part of the domain in correspondance to the MCS closest to the flight (MCS 1 in Fig. 1, top panel). It is difficult to assess if this can be attributed to the fact that outflow of MCS system (1) is not advected into the flight region or to the fact that BOLAM fails to reproduce the intensity and extent of this MCS system as mentioned in Sect. 3.1. BOLAM also shows the presence of saturated air (RH$_{ice}$>100%) in the lower layer (yellow shaded area) corresponding to main outflow altitudes.

Figure 7 shows the same set of diagnostics for 8 August. Although a similar picture to the previous event can be inferred, the number of trajectories uplifted by deep convection is larger during this event. Moreover, the fraction of air masses characterized

by lower t_c (16–24 h) is larger in the lower θ layer. Saturated air (yellow shade) is large and is present also in the upper layer but is located close to the outflow in the lower layer only.

The results for 11 August (Fig. 8) show much larger convective impact in both 354 and 367 K layers mostly related to uplift occuring in the large MCS labeled by (1) in Fig. 1 that is correctly reproduced by BOLAM (Fig. 5, lower panel). t_c ranges between 12 and 24 h at 354 K and has significantly higher values at 367 K, with a non-negligible number of trajectories with t_c ranging between 30 and 80 h. Both layers are characterized by large areas of saturated air.

The aerosol backscatter data from the Cloud-Aerosol Lidar and Infrared Pathfinder Satellite Observation (CALIPSO) that sampled the region where outflow occurred at longitude ranging between 3° E and 5° E on 11 August at 01:30 UTC (dashed line in Fig. 8, lower panel) are shown in Fig. 9. It shows a deck of solid particles up to 17 km (380 K) between 7° N and 18° N and vast deep convection area reaching up to 16 km (370 K) around 15° N. BOLAM trajectories give a coherent picture with regard to the convective ascent at the same time as the CALIPSO overpass and the presence of ice clouds in the outflow region between 15 km and the tropopause (located at 17 km) in the model results.

Overall, the analysis of cluster (1) shows that modeled convection has an important impact on the 353–355 K layer. At 363–366 K, convective transport influence is visible to a small extent on 7 and 8 August while the impact is much larger on 11 August. Moreover, the convective age (as given by t_c values) is variable showing that air masses influenced by very recent convection (t_c<24 h) coexist (especially at higher altitudes) with air masses influenced by older convection (t_c>48 h) which formed to the east over central Sahelian region above northern Nigeria and southern Chad.

5   Comparison with observations

We focus now on the vertical structure of convective outflow in the upper troposphere. In order to perform a comparison of the modeled and the observed vertical profiles, a set of diagnostics analogous to those described in Sect. 3.2 are applied to measurements: (1) f_{BSR} is the fraction of observations with BSR>1.2 and describes the vertical distribution of ice clouds to be compared with f_{ice}; (2) f_{CO_2} is the fraction of observations with CO_2 concentrations lower than the average value minus its standard deviation and describes the possible impact of deep convection on CO_2 profiles. f_{BSR} and f_{CO_2} were averaged over the same 12 θ-levels used for the model-based diagnostics discussed in the previous section. Vertical profiles of diagnostics are plotted in Fig. 10: model derived ones are colored in blue and observation-derived in red.

The vertical profile of f_{BSR} for 7 August flight (Fig. 10, upper panel, red dotted line) shows the presence of two distinct layers (below 360 K and at 367 K) as shown in Fig. 2. The model-derived vertical profiles of f_{ice} (left panel, solid blue line) and f_{ice}^c (left panel, dashed blue line) indicate that BOLAM predicts the presence of ice clouds in the lower layer that are formed inside air masses uplifted by deep convection. The BOLAM convective fraction, f_c (solid blue line on the right panel), decreases with height and is in acceptable agreement with f_{BSR} below 355 K (reported also in the right panels). Conversely, in the uppermost layer, where enhanced depolarization was observed, BOLAM does not reproduce ice clouds and reports a small (less than 3%) and old (up to 60 h) convective uplift. As discussed earlier, this could be due to the fact that BOLAM fails to fully reproduce the dynamics of the closest MCS to the flight for this event.

On 8 August (middle panel) the vertical structure of f_{BSR} is similar to the previous day but, in this case, BOLAM shows a better agreement throughout the entire vertical profile;,enhanced f_{ice} is simulated in correspondance to ice particle observations in the upper layer. f_{ice}^c is equal to f_{ice} below 355 K indicating that modelled ice clouds were formed in the convective outflow whilst above 355 K, the BOLAM model simulated ice particles in upper tropospheric air masses. Above 360 K t_c is characterized by values

Full Screen / Esc

Printer-friendly Version

Interactive Discussion

(48 h) larger than in the main outflow. In the same layer low CO_2 (shown in Fig. 3) was also observed and f_{CO_2} (red dashed line on the right panel) reaches 5%.

On 11 August (lower panel) the model shows two main ice cloud layers (below 360 K and at 370 K) in agreement with the observations which show distinct thin layers of ice particles. The trajectories overstimate f_{ice} with respect to f_{BSR}. 75% of model ice clouds are of recent convective origin in the lower layer (estimated as the ratio between f_{ice}^c and f_{ice} throughout the vertical range) whilst the fraction is around 30% in the upper layer. f_c shows a large convective fraction (up to 90%) which decreases with altitude. Air masses with higher t_c (72 to 90 h) are visible together with air masses originating from recent outflow (t_c less than 20 h) between 360 and 375 K. Within the same layer, f_{CO_2} is large (up to 90%) and corresponds to regions where low CO_2 was observed (see Fig. 3) .

The trajectory analysis shows that local convection hydrates the upper troposphere over West Africa and in one case (11 August) there is a significant impact up to 375 K. This recent convection is superimposed on older convection which took place up to 4 days before the observations. Even if a detailed analysis of cirrus formation mechanism is outside the scope of this paper, it is worth to noting that modelled and observed layers of ice particles are in good agreement, despite the fact that for the 11 August, the model overestimates the amount of ice clouds.

The analysis shows that ice particles are formed directly in the main outflow below 360 K and their presence is correlated to the uplift seen by model. Above the main outflow, trajectories indicates that ice clouds often form in the TTL at the top of mesoscale convective systems. These results are in qualitative agreement with a recent analysis of CALIPSO and CLOUDSAT observations which concluded that TTL cirrus are likely observed close to deep convective clouds (Sassen et al., 2009).

6 Conclusions

The analysis presented here aimed to characterize the impact of deep convection on the West African upper troposphere in August 2006 using a combination of aircraft data and mesoscale modelling. In particular, 3 M55 flights were analysed where there was a clear presence of organized convective systems either close to the flights or upwind over eastern and central Africa up to 4 days earlier.

On average, the observations of trace gases and aerosols collected during these flights on 7, 8 and 11 August, showed that it is possibile to identify a main convective outflow characterized by substantial hydration, low concentrations of CO_2 and O_3 and freshly nucleated ice particles. Deep convection largely determined the chemical composition up to a potential temperature level ranging between 355 K to 360 K that is assumed as top of the main outflow. These results confirm the outcomes presented in companion papers and, in particular those of Law (2010) based on estimations using trajectories calculated from large-scale meteorological analyses. Moreover, convective signature is often observed above the top of the main outflow up to the thermal tropopause (375 K) and can be identified by observations of thin ice cloud layers, enhanced fine particles concentration and CO_2 depletion. In particular, one specific event (11 August) clearly shows that the distributions of CO_2 and fine particles were strongly perturbed up to the tropical tropopause. On the other hand, large perturbations in ozone are not always observed since this region is characterized by land based convection that transports air masses containing different levels of ozone and its precursors or aerosols (local pollution, biomass burning, soil NO_x, lightning NO_x). As discussed further in Law (2010) large-scale westerly transport in the TTL can also bring air masses with marine convective signatures such as low O_3 into the UT over West Africa and this superposition of different sources makes it difficult to use ozone as a tracer of deep convective transport in this region.

Nudged mesoscale simulations performed with the BOLAM model correctly reproduce the general pattern of convection observed during the first 15 days of August 2006

Full Screen / Esc

Printer-friendly Version

Interactive Discussion

and therefore, can be used to estimate the convective outflow and to compared with the measurements. BOLAM shows good agreement with convective perturbation derived from observations of aerosol and chemical tracers for the main convective outflow region below 355 K and indicates that West Africa convection influences up to 50% of airmasses resulting in substantial hydration and formation of ice particles up to this level. BOLAM also correctly reproduces the outflow of a recent MSC on 11 August and simulates a large convective influence (up to 70%) between 355–370 K in agreement with the convective fraction estimated from observations of CO_2 and of freshly nucleated small particles.

Trajectories calculated from the mesoscale model simulation were used to estimate the convective age in order to identify when and where uplift occured. The time since convective uplift ranges between 18 and 24 h in the main convective layer but is more variable (between 20 and 96 h) above 355 K showing that deep convection in the central Sahel has a non negligible role in the uppermost troposphere, at least with respect to the formation of ice layers. The event of recent deep convection is characterized by the coexistence of air masses uplifted by recent and older convection; the last one being responsible of the presence of thin ice clouds. This is confirmed, at least on qualitative basis, by in-situ observations of CO_2, water vapour and aerosol that show the presence in the upper troposphere of perturbed trace gas concentrations, hydrated air, and particles that are not always measured in the same air masses. Air masses perturbed by more recent convection are likely characterized by depleted CO_2 and large concentrations of freshly nucleated particles whilst ozone shows concentrations slightly higher than in the mean convective outflow.

In-situ observations and model data helped to identify and quantify the role of deep convection in the TTL. Local convection generates a main outflow that is frequently present during measurement campaign. The impact on the atmospheric composition between main outflow and the tropopause is more difficult to assess due to different sources and the role of large-scale westerly transport processes. Nevertheless it is possibile to identify a clear signature of local convection in observations; model

aided analysis confirms the presence of direct injection up to the tropical tropopause by intense convective systems and indicates that composition is dependent on the residence time in the TTL after convective uplift. An interesting extension of this work, would be to implement the same analysis considering the whole monsoon season in order to characterize on a longer term (and larger scale) the impact of CENTRAL/West Africa convection on the UT. Climatological analysis of METEOSAT data (Laing et al., 2008) shows indeed that Sahelian cold clouds often forms in Nigeria, Chad and Sudan possibly feeded by chemicals from biomass burning sources (Mari et al., 2008; Real et al., 2009); extensive regional model simulations coupled with satellite data analysis would be necessary to quantify their effective impact on upper tropospheric composition.

References

Ancellet, G., Leclair de Bellevue, J., Mari, C., Nedelec, P., Kukui, A., Borbon, A., and Perros, P.: Effects of regional-scale and convective transports on tropospheric ozone chemistry revealed by aircraft observations during the wet season of the AMMA campaign, Atmos. Chem. Phys., 9, 383–411, 2009, http://www.atmos-chem-phys.net/9/383/2009/. 4930

Barret, B., Ricaud, P., Mari, C., Attié, J.-L., Bousserez, N., Josse, B., Le Flochmoën, E., Livesey, N. J., Massart, S., Peuch, V.-H., Piacentini, A., Sauvage, B., Thouret, V., and Cammas, J.-P.: Transport pathways of CO in the African upper troposphere during the monsoon season: a study based upon the assimilation of spaceborne observations, Atmos. Chem. Phys., 8,

3231–3246, 2008,
http://www.atmos-chem-phys.net/8/3231/2008/. 4930

Bertram, T. H., Perring, A. E., Woodridge, P. J., et al.: Direct measurements of the convective recycling of the upper troposphere, Science, 315(5813), 816–820, doi:10.1126/science.1134548, 2007. 4934, 4940

Buzzi, A. and Foschini, L.: Mesoscale meteorological features associated with heavy precipitation in the southern Alpine region, Meteorol. Atmos. Phys., 72, 131–146, 2000. 4938

Cairo, F., Di Donfrancesco, G., Adriani, A., Pulvirenti, L., and Fierli, F.: Comparison of Various Linear Depolarization Parameters Measured by Lidar Appl. Optics, 38(21), 4425–4432, 1999. 4934

Cairo, F., Pommereau, J. P., Law, K. S., Schlager, H., Garnier, A., Fierli, F., Ern, M., Streibel, M., Arabas, S., Borrmann, S., Berthelier, J. J., Blom, C., Christensen, T., D'Amato, F., Di Donfrancesco, G., Deshler, T., Diedhiou, A., Durry, G., Engelsen, O., Goutail, F., Harris, N. R. P., Kerstel, E. R. T., Khaykin, S., Konopka, P., Kylling, A., Larsen, N., Lebel, T., Liu, X., MacKenzie, A. R., Nielsen, J., Oulanowski, A., Parker, D. J., Pelon, J., Polcher, J., Pyle, J. A., Ravegnani, F., Rivière, E. D., Robinson, A. D., Röckmann, T., Schiller, C., Simões, F., Stefanutti, L., Stroh, F., Some, L., Siegmund, P., Sitnikov, N., Vernier, J. P., Volk, C. M., Voigt, C., von Hobe, M., Viciani, S., and Yushkov, V.: An overview of the SCOUT-AMMA stratospheric aircraft, balloons and sondes campaign in West Africa, August 2006: rationale, roadmap and highlights, Atmos. Chem. Phys. Discuss., 9, 19713–19781, 2009, http://www.atmos-chem-phys-discuss.net/9/19713/2009/. 4930, 4934

Corti, T., Luo, B. P., Fu, Q., Vömel, H., and Peter, T.: The impact of cirrus clouds on tropical troposphere-to-stratosphere transport, Atmos. Chem. Phys., 6, 2539–2547, 2006, http://www.atmos-chem-phys.net/6/2539/2006/. 4929

Corti, T., Luo, B. P., de Reus, M., et al.: Unprecedented evidence for deep convection hydrating the tropical stratosphere, Geophys. Res. Lett., 35, L10810, doi:10.1029/2008GL033641, 2008. 4930

Chaboureau, J.-P., Cammas, J.-P., Duron, J., Mascart, P. J., Sitnikov, N. M., and Voessing, H.-J.: A numerical study of tropical cross-tropopause transport by convective overshoots, Atmos. Chem. Phys., 7, 1731–1740, 2007, http://www.atmos-chem-phys.net/7/1731/2007/. 4930

Curtius, J.: Nucleation of atmospheric particles, C. R. Phys., 7, 1027–1045, 2006. 4934

Impact of deep convection in the TTL in West Africa

F. Fierli et al.

Dessler, A. E.: The effect of deep, tropical convection on the tropical tropopause layer, J. Geophys. Res., 107(D3), 4033, doi:10.1029/2001JD000511, 2002. 4930

Fierli, F., Di Donfrancesco, G., Cairo, F., Marécal, V., Zampieri, M., Orlandi, E., and Durry, G.: Variability of cirrus clouds in a convective outflow during the Hibiscus campaign, Atmos. Chem. Phys., 8, 4547–4558, 2008, http://www.atmos-chem-phys.net/8/4547/2008/. 4939

Folkins, I. and Martin, R. V.: The vertical structure of tropical convection and its impact on the budgets of water vapor and ozone, J. Atmos. Sci., 62, 1560–1573, 2005. 4929

Fueglistaler, S. and Fu, Q.: Impact of clouds on radiative heating rates in the tropical lower stratosphere, J. Geophys. Res., 111, D23202, doi:10.1029/2006JD007273, 2006. 4929

Fueglistaler, S., Dessler, A. E., Dunkerton, T. J., Folkins, I., Fu, Q., and Mote, P. W.: Tropical tropopause layer, Rev. Geophys., 47, RG1004, doi:10.1029/2008RG000267, 2009. 4929

Gheusi, F. and Stein, J.: Lagrangian description of airflows using Eulerian passive tracers, Q. J. Roy. Meteor. Soc., 128(579), 337–360, 2002. 4939

Homan, C. D., Volk, C. M., Kuhn, A. C., Werner, A., Baehr, J., Viciani, S., Ulanovski, A., and Ravegnani, F.: Tracer measurements in the tropical tropopause layer during the AMMA/SCOUT-O3 aircraft campaign, Atmos. Chem. Phys. Discuss., 9, 25049–25084, 2009, http://www.atmos-chem-phys-discuss.net/9/25049/2009/. 4935

Janicot, S., Thorncroft, C. D., Ali, A., Asencio, N., Berry, G., Bock, O., Bourles, B., Caniaux, G., Chauvin, F., Deme, A., Kergoat, L., Lafore, J.-P., Lavaysse, C., Lebel, T., Marticorena, B., Mounier, F., Nedelec, P., Redelsperger, J.-L., Ravegnani, F., Reeves, C. E., Roca, R., de Rosnay, P., Schlager, H., Sultan, B., Tomasini, M., Ulanovsky, A., and ACMAD forecasters team: Large-scale overview of the summer monsoon over West Africa during the AMMA field experiment in 2006, Ann. Geophys., 26, 2569–2595, 2008, http://www.ann-geophys.net/26/2569/2008/. 4930

Kain, J. S.: The Kain-Fritsch convective parametrization: an update, J. Appl. Meteorol., 43, 170–181, 2004. 4937

Khaykin, S., Pommereau, J.-P., Korshunov, L., Yushkov, V., Nielsen, J., Larsen, N., Christensen, T., Garnier, A., Lukyanov, A., and Williams, E.: Hydration of the lower stratosphere by ice crystal geysers over land convective systems, Atmos. Chem. Phys., 9, 2275–2287, 2009, http://www.atmos-chem-phys.net/9/2275/2009/. 4930

Title Page

Abstract | Introduction

Conclusions | References

Tables | Figures

⏮ | ⏭

◀ | ▶

Back | Close

Full Screen / Esc

Printer-friendly Version

Interactive Discussion

Laing, A. G., Carbone, R., Levizzani, V., and Tuttle, J.: The propagation and diurnal cycles of deep convection in northern tropical Africa, Q. J. Roy. Meteor. Soc., 134, 93–109, doi:10002/qj.194, 2008. 4947

Mace, G. G., Benson, S., and Vernon, E.: Cirrus Clouds and the Large-Scale Atmospheric State: Relationships Revealed by Six Years of Ground-Based Data, J. Climate, 19, 3257–3278, doi:10.1175/JCLI3786.1, 2006. 4934

Mari, C. H., Cailley, G., Corre, L., Saunois, M., Attié, J. L., Thouret, V., and Stohl, A.: Tracing biomass burning plumes from the Southern Hemisphere during the AMMA 2006 wet season experiment, Atmos. Chem. Phys., 8, 3951–3961, 2008,
http://www.atmos-chem-phys.net/8/3951/2008/. 4931, 4947

Marti, L. and Mauersberger, K.: A survey and new measurements of ice vapor pressure at temperatures between 170 and 250 K, Geophys. Res. Lett., 20, 363–366, 1993. 4934

Morcrette, J. J., Clough, S. A., Mlawer, E. J., and Iacono, M. J.: Impact of a validated radiative transfer scheme, RRTM, on the ECMWF model climate and 10-day forecasts, ECMWF Technical Memo, 252, 1998. 4938

Mullendore, G. L., Durran, D. R., and Holton, J. R.: Cross.tropopause tracer transport in mid-latitude convection, J. Geophys. Res., 116, D06113, doi:10.129/2004JD005059, 2005. 4940

Park, S., Jiménez, R., Daube, B. C., Pfister, L., Conway, T. J., Gottlieb, E. W., Chow, V. Y., Curran, D. J., Matross, D. M., Bright, A., Atlas, E. L., Bui, T. P., Gao, R.-S., Twohy, C. H., and Wofsy, S. C.: The CO_2 tracer clock for the Tropical Tropopause Layer, Atmos. Chem. Phys., 7, 3989–4000, 2007,
http://www.atmos-chem-phys.net/7/3989/2007/. 4936

Pfister, L., Selkirk, H. B., Jensen, E. J., et al.: Aircraft observations of thin cirrus clouds near the tropical tropopause, J. Geophys. Res., 106(D9), 9765–9786, 2001. 4934

Real, E., Orlandi, E., Law, K. S., Fierli, F., Josset, D., Cairo, F., Schlager, H., Borrmann, S., Kunkel, D., Volk, M., McQuaid, J. B., Stewart, D. J., Lee, J., Lewis, A., Hopkins, J. R., Ravegnani, F., Ulanovski, A., and Liousse, C.: Cross-hemispheric transport of central African biomass burning pollutants: implications for downwind ozone production, Atmos. Chem. Phys. Discuss., 9, 17385–17427, 2009,
http://www.atmos-chem-phys-discuss.net/9/17385/2009/. 4931, 4947

Redelsperger, J. L., Thorncroft, C., Diedhiou, A., Lebel, T., Parker, D. J., and Polcher, J.: African Monsoon Multidisciplinary Analysis (AMMA): An International Research Project and Field Campaign, B. Am. Meteor. Soc., 87(12), 1739-1746, 2006. 4930

Impact of deep convection in the TTL in West Africa

F. Fierli et al.

Ritter, B. and Geleyn, J.: A comprehensive radiation scheme for numerical weather prediction models with potential applications in climate simulations, Mon. Weather Rev., 120, 303–325, 1992. 4938

Sassen, K., Wang, Z. and Liu, D.: Cirrus clouds and deep convection in the tropics: Insights from CALIPSO end CloudSat, J. Geophys. Res., 114, D00H06, doi:10.129/2009JD011916, 2009. 4944

Saunders, R. and Brunel, P.: RTTOV-8 user guide, UK Met. offfice publication, NPWSAF-MO-UD-008, 45, 2005. 4938

Saunois, M., Reeves, C. E., Mari, C. H., Murphy, J. G., Stewart, D. J., Mills, G. P., Oram, D. E., and Purvis, R. M.: Factors controlling the distribution of ozone in the West African lower troposphere during the AMMA (African Monsoon Multidisciplinary Analysis) wet season campaign, Atmos. Chem. Phys., 9, 6135–6155, 2009, http://www.atmos-chem-phys.net/9/6135/2009/. 4931

Schmetz, J., Tjemkes, S. A., Gube, M., and van de Berg, L.: Monitoring deep convection and convective overshooting with METEOSAT, Proceedings of the A0.1 Symposium of COSPAR Scientific Commission A, Adv. Space Res., 19(3), 433–441, 1997. 4932

Schiller, C., Grooß, J.-U., Konopka, P., Plöger, F., Silva dos Santos, F. H., and Spelten, N.: Hydration and dehydration at the tropical tropopause, Atmos. Chem. Phys., 9, 9647–9660, 2009, http://www.atmos-chem-phys.net/9/9647/2009/. 4931

Stewart, D. J., Taylor, C. M., Reeves, C. E., and McQuaid, J. B.: Biogenic nitrogen oxide emissions from soils: impact on NO_x and ozone over west Africa during AMMA (African Monsoon Multidisciplinary Analysis): observational study, Atmos. Chem. Phys., 8, 2285–2297, 2008, http://www.atmos-chem-phys.net/8/2285/2008/. 4931

Impact of deep convection in the TTL in West Africa

F. Fierli et al.

Title Page

Abstract | Introduction

Conclusions | References

Tables | Figures

◄ | ►►

◄ | ►

Back | Close

Full Screen / Esc

Printer-friendly Version

Interactive Discussion
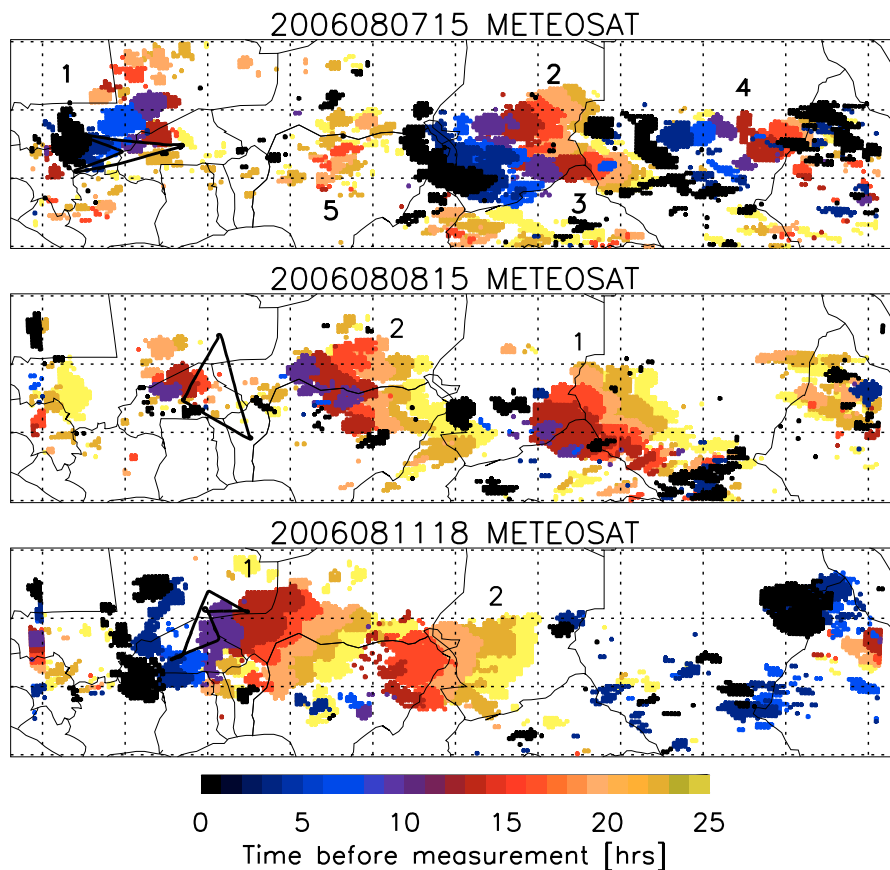
**Fig. 1.** Meteosat Cloud top brightness temperature time evolution during 24 h prior to the M55 flight on 7 August 2006 (top panel), 8 August 2006 (middle level), and 11 August 2006 (lower panel). Clouds are shown as colored regions where CTBT<210 K. Colors indicates the time (in hours) prior to observations. Flight path is shown by the black line; numbers identify different MSCs described in the text.
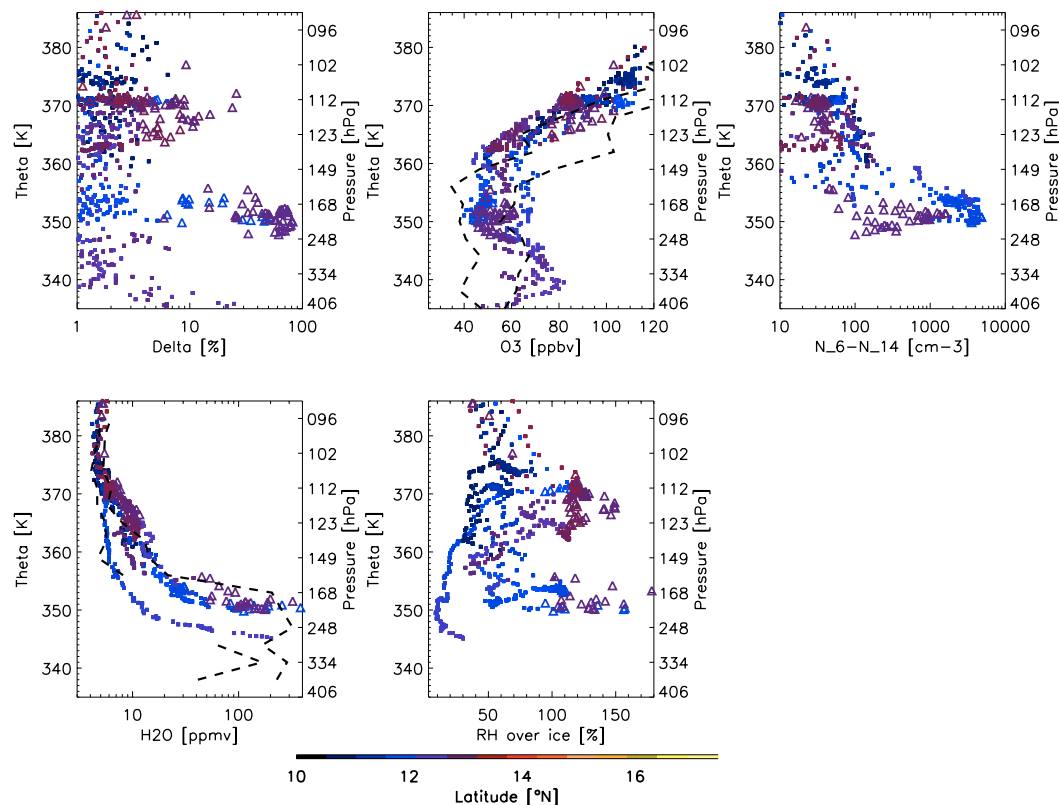
Fig. 2. Vertical profiles of observed depolarization D ozone O_3, particle fine fraction N_6–N_{14}, water vapour H_2O and relative humidity with respect to ice RHI on 7 August 2006. Colors indicate the measurement latitude; triangles indicate the observations within air parcels containing aerosol (BSR>1.2). Dashed lines indicates average non-convective profile ± one standard deviation of for O_3, CO_2 and H_2O (see text for details).
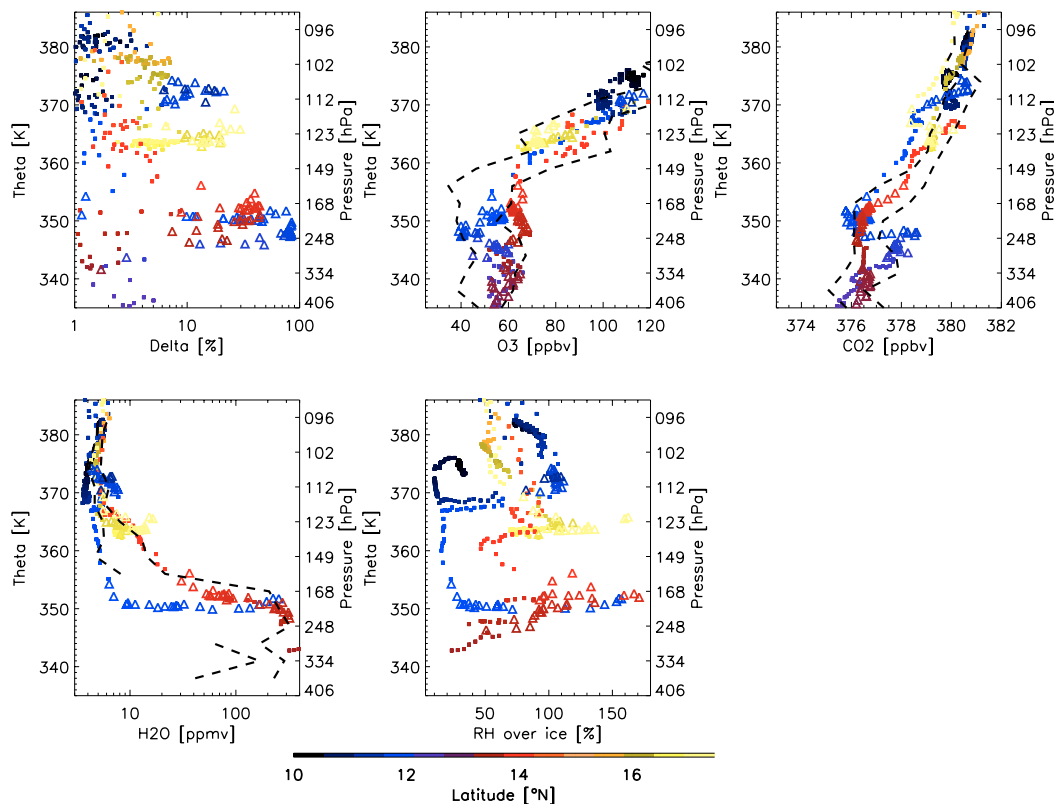
Fig. 3. As Fig. 2 but for D, O_3, carbon dioxide (CO_2), N_6–N_{14}, H_2O and RHI on 8 August 2006. Particle fine fraction N_6–N_{14} observations are too sparse to allow to reconstruct a vertical profile.
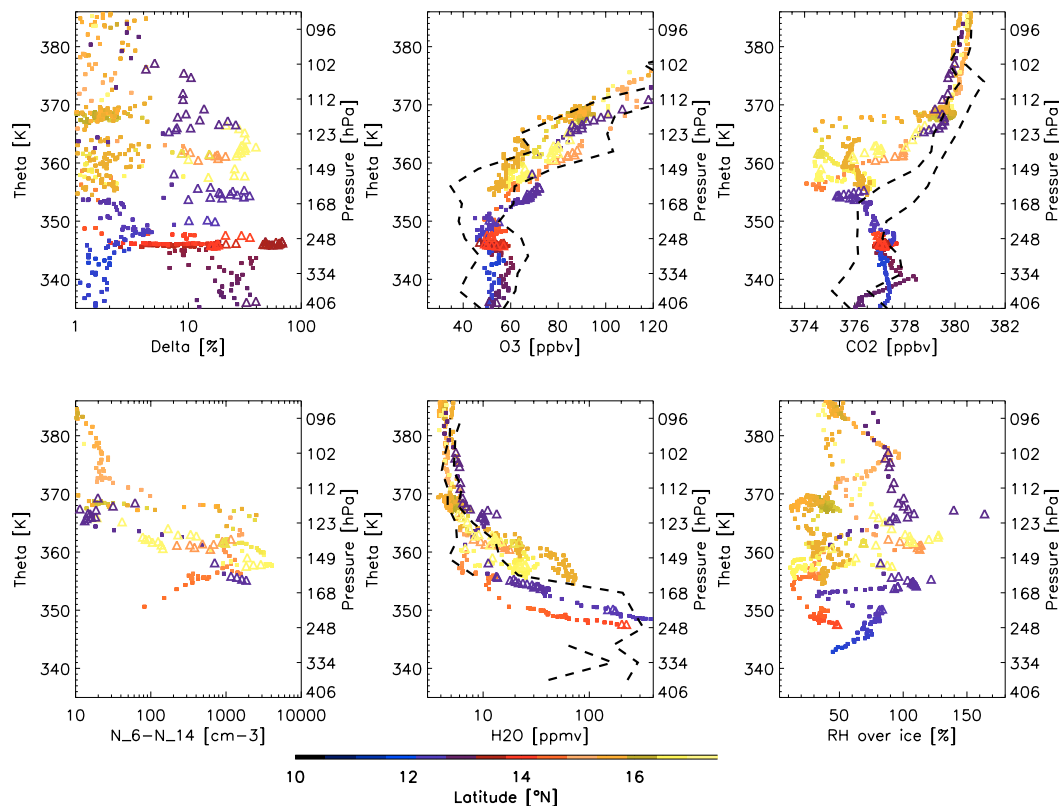
Fig. 4. As Fig. 2 but D, O_3, CO_2, H_2O and RHI on 11 August 2006.

⏮ | ⏭

◀ | ▶

Back | Close

Full Screen / Esc

Printer-friendly Version

Interactive Discussion
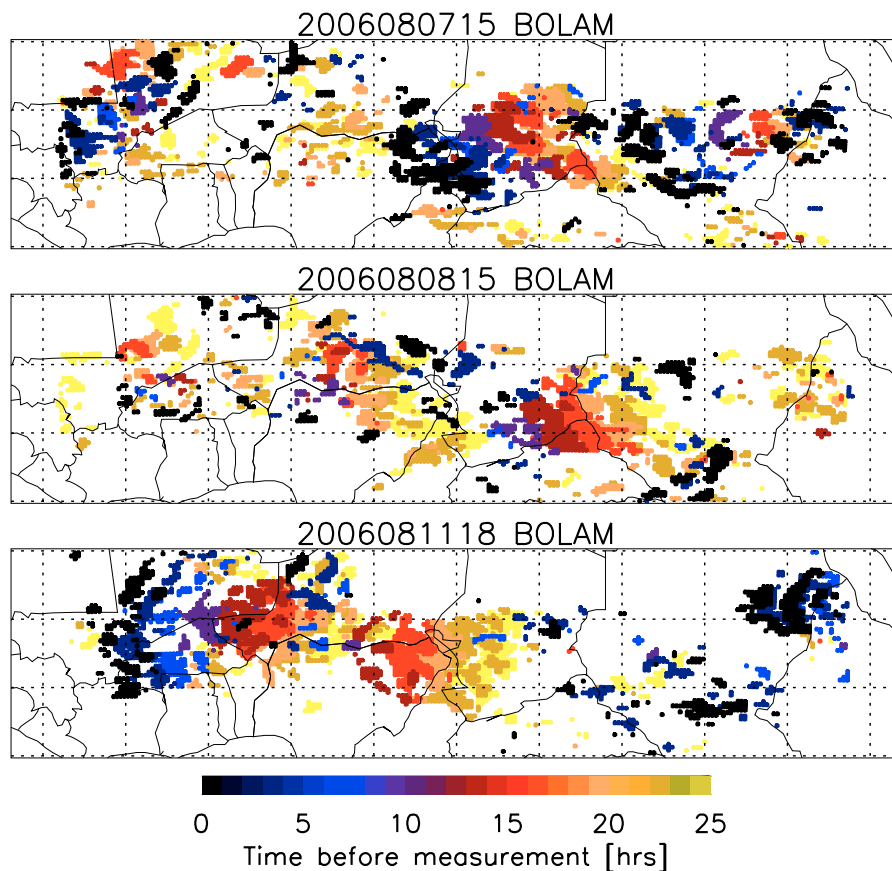
Fig. 5. As Fig. 1 but for the BOLAM model.
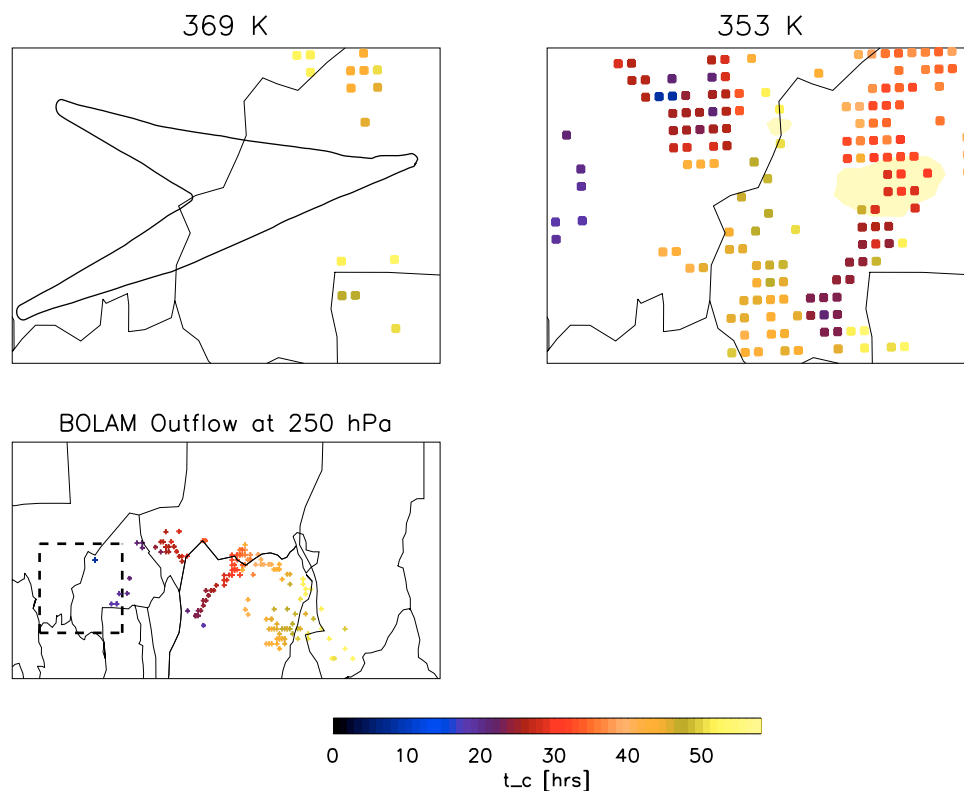
Fig. 6. Above: maps of t_c estimated from the BOLAM trajectories (see text for definition) for two theta layers (368–369 K above the main convective levels and at 353–355 K) for 7 August 2009. Yellow shaded area indicates where BOLAM RH$_{ice}$ exceeds 100%. The flight path is also reported in the top left panel. Below: the position where air parcels crosses irreversibly the 250 hPa surface. Dashed box indicate the horizontal domain shown above where trajectories in cluster 1 (see text) originates. Colors indicate t_c
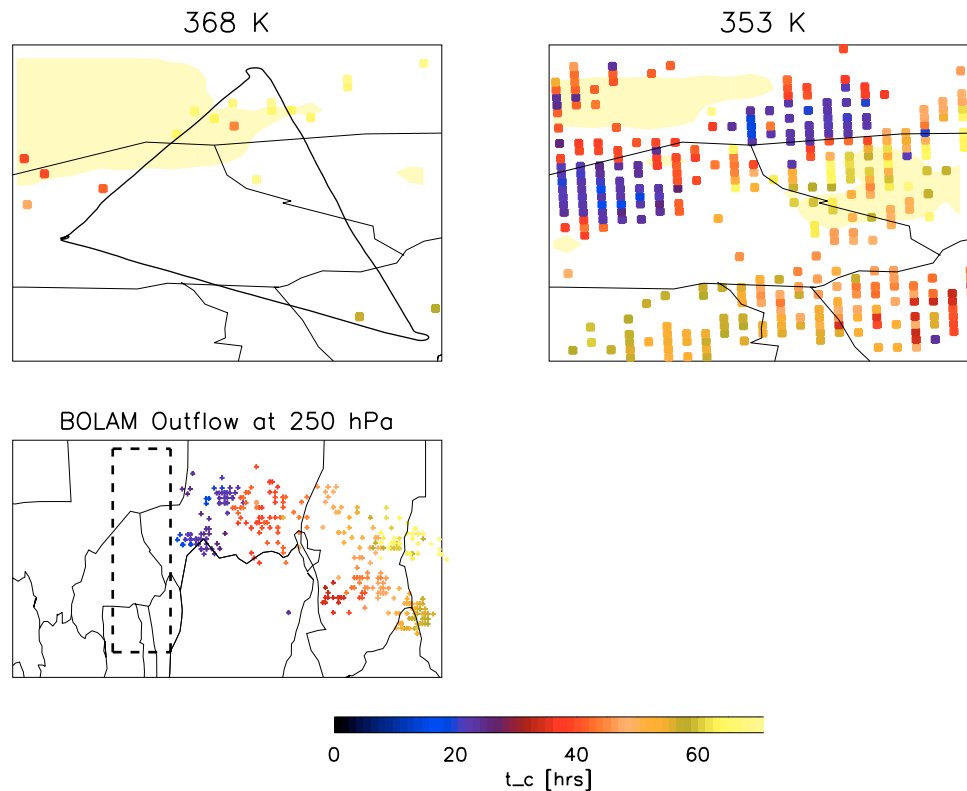
Fig. 7. As Fig. 6 but for the 8 August 2006 flight.
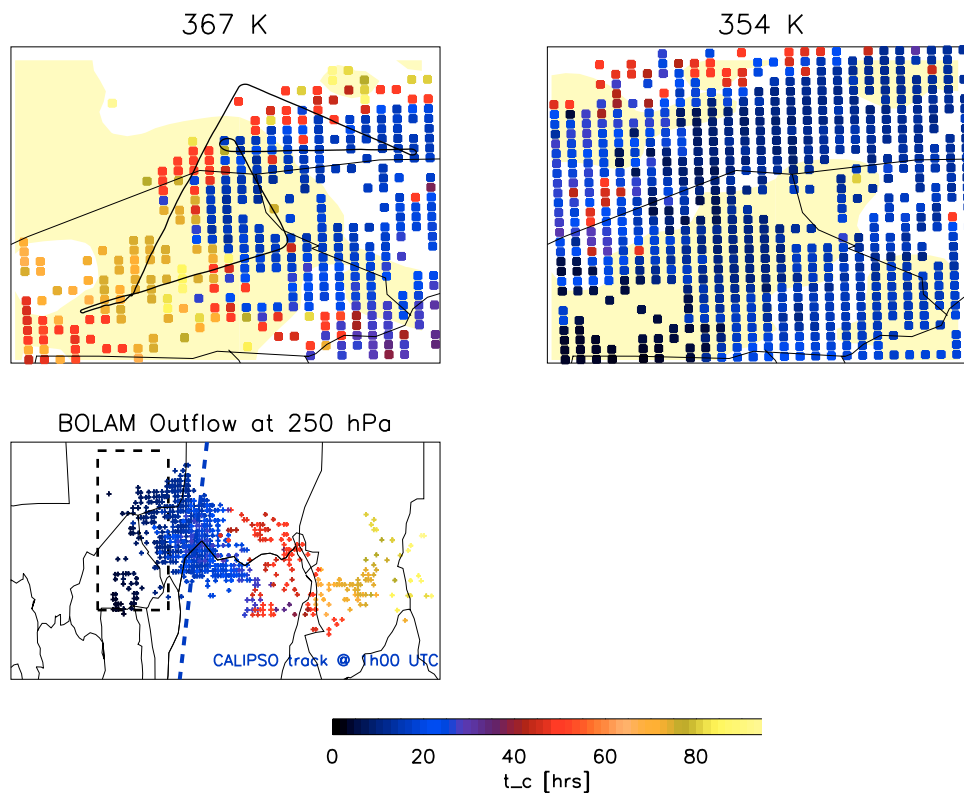
Fig. 8. As Fig. 6 but for the 11 August 2006 flight. Dashed line indicates CALIPSO overpass and blue color follows the t_c scale (15 h before the measurement).
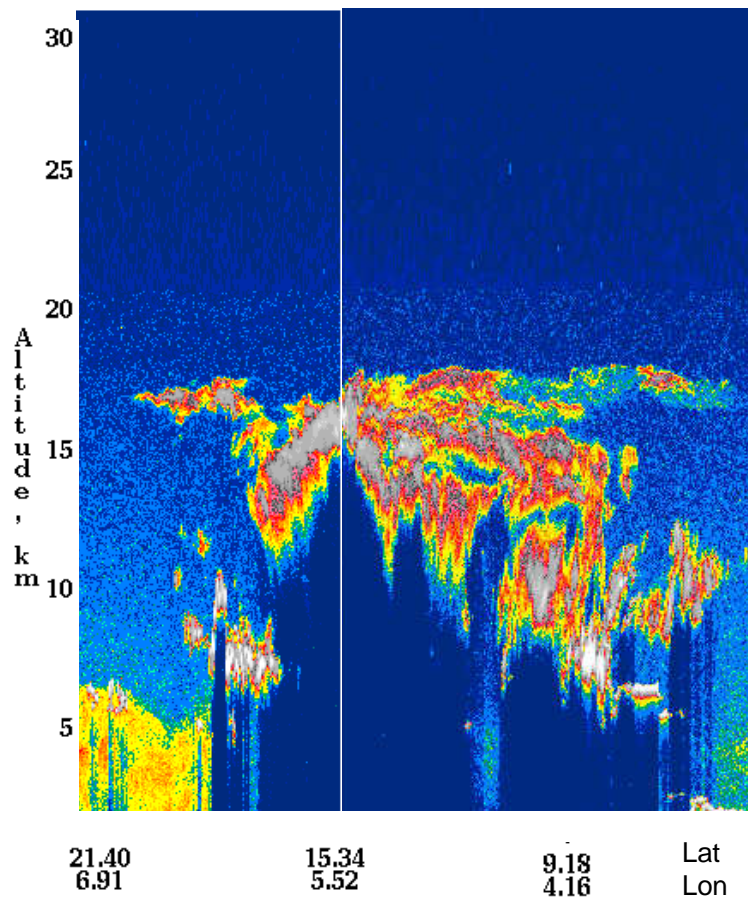
Fig. 9. CALIPSO aerosol backscatter observed at 01:30 UTC on 11 August. Aerosol observations (not shown) shows that aerosol are in solid phase.
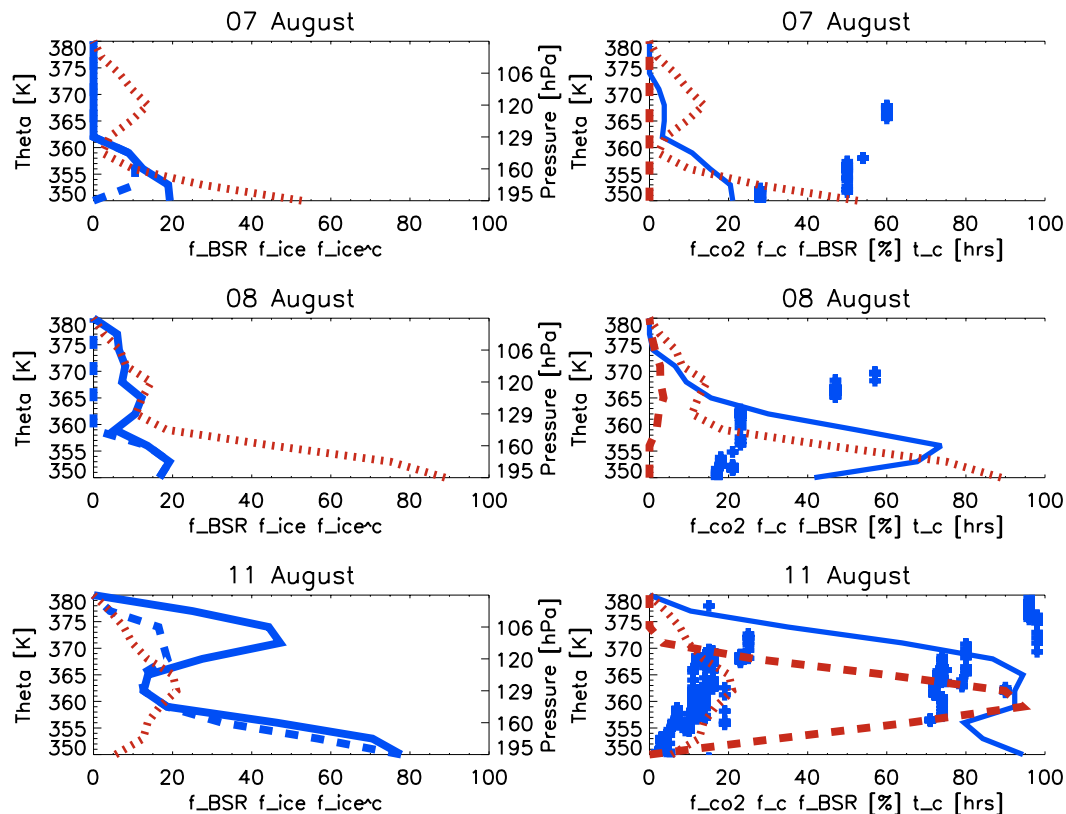
Fig. 10. Vertical profiles of the diagnostics described in the text. Model-derived ones are plotted in blue, observation-derived in red. Left column: BOLAM ice fraction f_{mice} (solid blue line) and convective ice fraction f_{ice}^c (dashed blue line); observed aerosol fraction f_{BSR} (dotted red line), Right column: BOLAM convective time t_c (blue symbols), convective fraction f_c; observed fraction of outliars in $CO_2 f_{CO_2}$ plotted as dashed red line; f_{BSR} is also plotted to be compared with f_c. Top panels are for 7 August middle for 8 August and bottom for 11 August.

[ACPD](#)

10, 4927–4961, 2010

Impact of deep convection in the TTL in West Africa

F. Fierli et al.

Title Page	
Abstract	Introduction
Conclusions	References
Tables	Figures
◀	▶
◀	▶
Back	Close
Full Screen / Esc	
Printer-friendly Version	
Interactive Discussion	